

Cluster Compounds

cyclo-Ti₃[$\eta^2(\mu_2\text{-C,O})$]₃: A Side-on-Bonded Polycarbonyl Titanium Cluster with Potentially Antiaromatic Character***Qiang Xu,* Ling Jiang, and Nobuko Tsumori*

Carbon monoxide, one of the most important ligands in transition-metal chemistry from an academic and industrial viewpoint, is well known to coordinate only in the direction from the C atom to metal(s), forming terminal or bridging metal–CO bonds, in the known metal carbonyls,^[1] with very few exceptions for chemisorbed CO on some transition metal

[*] Prof. Dr. Q. Xu, L. Jiang
National Institute of Advanced Industrial Science and Technology (AIST)
Ikeda, Osaka 563-8577 (Japan)
and
Graduate School of Science and Technology
Kobe University
Nada Ku, Kobe, Hyogo 657-8501 (Japan)
Fax: (+81) 72-751-9629
E-mail: q.xu@aist.go.jp

Dr. N. Tsumori
National Institute of Advanced Industrial Science and Technology (AIST)
Ikeda, Osaka 563-8577 (Japan)
and
Toyama National College of Technology
13 Hongo-machi, Toyama, 939-8630 (Japan)

[**] We gratefully thank Dr. K. Ohta for helpful discussion and the referees for valuable comments and suggestions, and acknowledge AIST and Kobe University for financial support.



Supporting information for this article is available on the WWW under <http://www.angewandte.org> or from the author.

surfaces^[2] and so-called four-electron-donor CO in a limited number of organometallic complexes.^[3] The recently reported $\text{Sc}_2[\eta^2(\mu_2\text{-C}_2\text{O})]$ is a simple homoleptic metal carbonyl with only a single side-on-bonded CO ligand,^[4] whereas there has been no report thus far of a side-on-bonded polycarbonyl metal cluster. Here we report the generation, IR spectroscopic characterization, and theoretical investigation of side-on-bonded mono- and polycarbonyl titanium clusters $\text{Ti}_2(\text{CO})_n$ ($n=1, 2$) and $\text{Ti}_3(\text{CO})_n$ ($n=1-3$). In particular, calculations revealed the novel planar, CO side-on-bonded windmill-like *cyclo*- $\text{Ti}_3[\eta^2(\mu_2\text{-C}_2\text{O})]_3$ molecule, which may have antiaromatic character.

Matrix-isolated $\text{Ti}_2(\text{CO})_n$ ($n=1, 2$) and $\text{Ti}_3(\text{CO})_n$ ($n=1-3$) molecules were produced by codeposition of laser-ablated Ti atoms with CO in excess argon at 7 K and were investigated by FTIR spectroscopy.^[5] Recent studies, with the aid of an isotopic substitution technique, have shown that a combination of matrix-isolation IR spectroscopy and quantum chemical calculations is a powerful tool for investigating the spectrum, structure, and bonding of novel species.^[6,7] The IR spectra as a function of changes in CO concentrations and laser energy are of particular interest here. At high CO concentration (0.20%) and low laser energy (4 mJ/pulse), only mononuclear species $\text{Ti}(\text{CO})_n$ ($n=1-6$) with IR absorptions in the 1740–2040 cm^{-1} region were observed as the reaction products on sample annealing,^[8] which have been previously identified.^[9] At lower CO concentration (0.05%) and higher laser power (12 mJ/pulse), these mononuclear species almost disappeared, while new absorptions appeared in the 1160–1420 cm^{-1} region on sample annealing, which disappeared after broadband irradiation and did not recover upon further annealing (Figure 1 and Table 1).^[8] Note that these new bands were only observed with lower CO concentration and higher laser energy than those for the mononuclear Ti carbonyls, that is, these new products involve more than one Ti atom. Since doping with CCl_4 as an electron scavenger had no effect on these bands, the products are neutral (Figure 1).

On the basis of the growth/decay characteristics as a function of changes in experimental conditions (Figure 1 and ref. [8]), the bands in the 1160–1420 cm^{-1} region can be grouped into five species. All of the absorptions exhibit the isotopic $^{12}\text{C}^{16}\text{O}/^{13}\text{C}^{16}\text{O}$ and $^{12}\text{C}^{16}\text{O}/^{12}\text{C}^{18}\text{O}$ frequency ratios characteristic of C–O stretching vibrations, but their $\nu_{\text{C-O}}$ values are anomalously lower than for terminal or bridging CO (Table 1 and Table 2). They are therefore attributed to Ti cluster carbonyls containing only side-on-bonded CO ligand(s) with extremely weakened C–O bonding, as observed for $\text{Sc}_2[\eta^2(\mu_2\text{-C}_2\text{O})]$.^[4] The absorptions at 1297.8 cm^{-1} (trapping sites: 1304.2 and 1293.5 cm^{-1}) and at 1253.3 cm^{-1} respectively split into doublets for the mixed

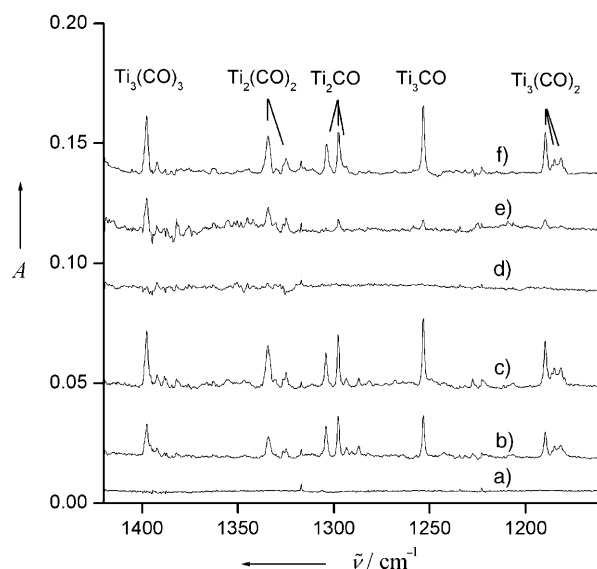


Figure 1. IR spectra in the 1420–1160 cm^{-1} region for laser-ablated Ti atoms codeposited with 0.05% CO in argon at 7 K: a) after 60 min of sample deposition, b) after annealing to 30 K, c) after annealing to 34 K, d) after 20 min of broadband irradiation, e) after annealing to 36 K, f) after doping with 0.01% CCl_4 and annealing to 34 K.

Table 1: IR absorptions [cm^{-1}] observed from codeposition of laser-ablated Ti atoms with CO in an excess of argon at 7 K.

$^{12}\text{C}^{16}\text{O}$	$^{13}\text{C}^{16}\text{O}$	$^{12}\text{C}^{18}\text{O}$	$^{12}\text{C}^{16}\text{O} + ^{13}\text{C}^{16}\text{O}$	$^{12}\text{C}^{16}\text{O} + ^{12}\text{C}^{18}\text{O}$	Assignment
1397.6	1365.1	1368.7	1397.6, 1388.7, 1380.6, 1365.1	1397.6, 1388.4, 1381.8, 1368.5	$\text{Ti}_3(\text{CO})_3$
1334.3	1303.4	1307.4	1334.3, 1315.8, 1303.8	1334.2, 1318.5, 1307.0	$\text{Ti}_2(\text{CO})_2$
1324.8	1294.2	1298.8			$\text{Ti}_2(\text{CO})_2$ site
1304.2	1274.2	1277.6	1304.2, 1274.4	1304.0, 1277.6	Ti_2CO site
1297.8	1268.2	1271.4	1297.7, 1268.3	1297.7, 1271.4	Ti_2CO
1293.5	1264.4	1267.5	1293.3, 1264.2	1293.3, 1267.2	Ti_2CO site
1253.3	1224.8	1228.8	1253.3, 1224.8	1253.4, 1228.7	Ti_3CO
1189.9	1162.2	1165.2	1190.0, 1172.8, 1164.1 (1231.5)	1189.9, 1173.6, 1165.0 (1235.1)	$\text{Ti}_3(\text{CO})_2$
1185.0	1157.3	1159.7			$\text{Ti}_3(\text{CO})_2$ site
1181.7	1154.2	1157.2			$\text{Ti}_3(\text{CO})_2$ site

Table 2: Comparison of observed and calculated isotopic frequency ratios of the reaction products.

Molecule	Mode	$^{12}\text{C}^{16}\text{O}/^{13}\text{C}^{16}\text{O}$			$^{12}\text{C}^{16}\text{O}/^{12}\text{C}^{18}\text{O}$		
		obsd	BP86	B3LYP	obsd	BP86	B3LYP
Ti_2CO	C–O str.	1.0233	1.0238	1.0237	1.0208	1.0222	1.0223
$\text{Ti}_2(\text{CO})_2$	C–O asym. str.	1.0237	1.0239	1.0236	1.0206	1.0217	1.0223
Ti_3CO	C–O str.	1.0233	1.0241	1.0236	1.0199	1.0217	1.0225
$\text{Ti}_3(\text{CO})_2$	C–O asym. str.	1.0238	1.0240	1.0237	1.0212	1.0219	1.0225
$\text{Ti}_3(\text{CO})_3$	C–O asym. str.	1.0238	1.0261	1.0240	1.0211	1.0238	1.0217

$^{12}\text{C}^{16}\text{O} + ^{13}\text{C}^{16}\text{O}$ and $^{12}\text{C}^{16}\text{O} + ^{12}\text{C}^{18}\text{O}$ samples (Figure 2), and this indicates that only one CO subunit is involved in each molecule;^[10] the former is assigned to Ti_2CO and the latter to Ti_3CO on the basis of the stepwise annealing behavior (Figure 1). The absorptions at 1334.3 cm^{-1} (site: 1324.8 cm^{-1}) and at 1189.9 cm^{-1} (sites: 1185.0 and 1181.7 cm^{-1}) respectively split into triplets with approxi-

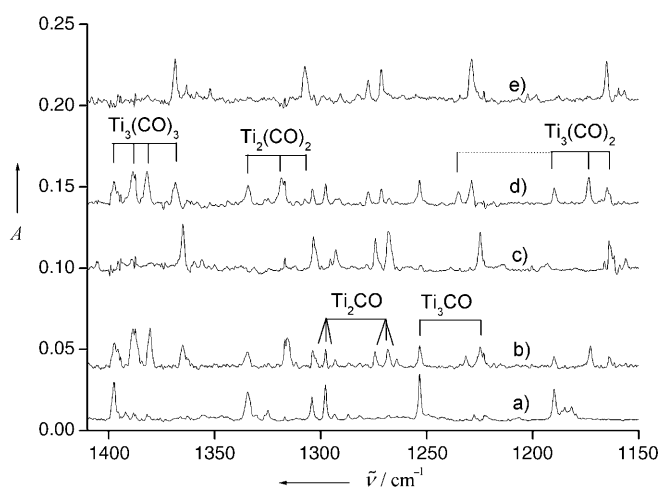


Figure 2. IR spectra in the 1420–1150 cm^{-1} region for laser-ablated Ti atoms codeposited with isotopic CO in Ar for 60 min at 7 K, followed by annealing to 34 K. a) 0.05% $^{12}\text{C}^{16}\text{O}$, b) 0.025% $^{12}\text{C}^{16}\text{O}$ + 0.025% $^{13}\text{C}^{16}\text{O}$, c) 0.05% $^{13}\text{C}^{16}\text{O}$, d) 0.025% $^{12}\text{C}^{16}\text{O}$ + 0.025% $^{12}\text{C}^{18}\text{O}$, e) 0.05% $^{12}\text{C}^{18}\text{O}$.

mately 1:2:1 relative intensities in the mixed-isotope experiments (Figure 2), that is, each mode involves two equivalent CO ligands;^[10] we assign the former to the asymmetric C–O stretching of $\text{Ti}_2(\text{CO})_2$, and the latter to $\text{Ti}_3(\text{CO})_2$. The splitting of the highest absorption at 1397.6 cm^{-1} into a quadruplet in the mixed-isotope experiments suggests the involvement of three CO subunits.^[10] Quantum chemical calculations (vide infra) indicate that this species is preferably assigned to $\text{Ti}_3(\text{CO})_3$, rather than to $\text{Ti}_2(\text{CO})_3$. For species containing two or three CO ligands, symmetric C–O stretching modes should be observed due to the reduced symmetry of the isotopically mixed species. The symmetric C–O stretching for each isotopomer of $\text{Ti}_2(^{12}\text{C}^{16}\text{O})$ -($^{13}\text{C}^{16}\text{O}$) and $\text{Ti}_2(^{12}\text{C}^{16}\text{O})$ ($^{12}\text{C}^{18}\text{O}$) overlapped with $\text{Ti}_3(\text{CO})_3$ absorptions, and the symmetric C–O stretching modes in the mixed-isotope spectra for $\text{Ti}_3(\text{CO})_3$ were too weak to be observed, as predicted by DFT calculations,^[8] whereas an additional blue-shifted absorption was observed for the symmetric C–O stretching mode for each isotopomer of $\text{Ti}_3(^{12}\text{C}^{16}\text{O})$ ($^{13}\text{C}^{16}\text{O}$) and $\text{Ti}_3(^{12}\text{C}^{16}\text{O})$ ($^{12}\text{C}^{18}\text{O}$) (Table 1). With 0.05% CO all five species were observed, whereas only the CO-poorer and Ti-richer species, Ti_2CO and Ti_3CO , survived on further lowering the CO concentration to 0.02%.^[8]

Density functional calculations, performed at the BP86/6-311++G(d,p) and B3LYP/6-311++G(d,p) levels^[11] for the possible isomers of $\text{Ti}_2(\text{CO})_n$ ($n = 1, 2$) and $\text{Ti}_3(\text{CO})_n$ ($n = 1-3$), provide strong support to the above assignments and insight into structures and bonding. The trial calculations to test reliability gave $\nu_{\text{C-O}}$ values for linear quintet TiCO of 1889.0 (BP86) and 1971.2 cm^{-1} (B3LYP), close to the experimental value (1855.2 cm^{-1}) with scale factors (obsd/

calcd frequency ratios) of 0.982 and 0.941, respectively, in good agreement with previous reports ($\nu_{\text{C-O}} = 1854.4\text{ cm}^{-1}$ in solid argon, 1920.0 cm^{-1} in solid neon).^[9] Hereafter, mainly BP86 results are presented for discussion. The calculations show that the planar $\text{Ti}_2[\eta^2(\mu_2\text{-C,O})]$ (**1**) molecule with a single side-on-bonded CO ligand, similar to $\text{Sc}_2[\eta^2(\mu_2\text{-C,O})]$,^[4] and the planar $\text{Ti}_2[\eta^2(\mu_2\text{-C,O})]_2$ (**2**) molecule with two side-on-bonded CO units (Figure 3) nicely match the experimental vibrational frequencies, relative absorption intensities, and isotopic shifts for $\text{Ti}_2(\text{CO})$ and $\text{Ti}_2(\text{CO})_2$, respectively. The $\nu_{\text{C-O}}$ values of **1** and **2** are predicted to be 1330.9 and 1332.6 cm^{-1} (B_2), respectively, in good agreement with observations (1297.8 and 1334.3 cm^{-1}), whereas the symmetric C–O stretching mode (A_1) of **2** exhibits a much lower intensity than the antisymmetric B_2 mode (Table S1 in Supporting Information), consistent with the absence of this A_1 absorption in the IR spectra. The calculated $^{12}\text{C}^{16}\text{O}/^{13}\text{C}^{16}\text{O}$ ($^{12}\text{C}^{16}\text{O}/^{12}\text{C}^{18}\text{O}$) frequency ratios of **1** and **2** are 1.0238 (1.0222) and 1.0239 (1.0217), respectively, in accord with the observed values of 1.0233 (1.0208) and 1.0237 (1.0206) (Table 2). Our

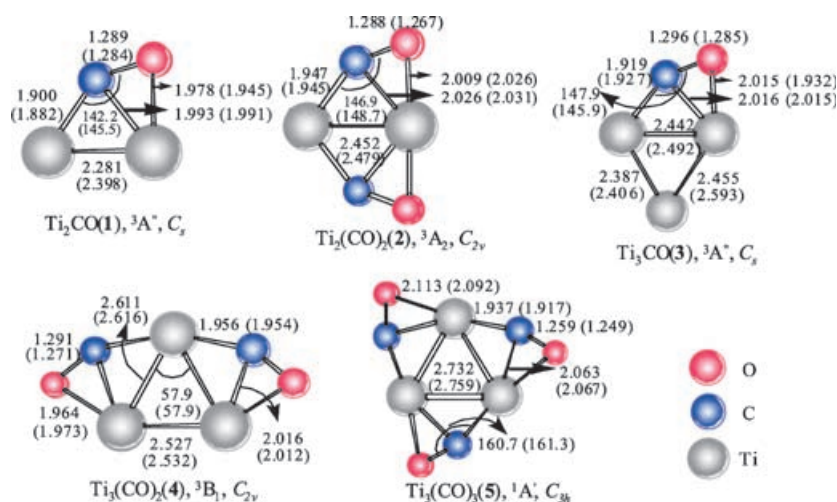


Figure 3. Optimized structures (bond lengths in Å, bond angles in degrees), electronic ground states, and point groups of the reaction products calculated at the BP86/6-311++G(d,p) and B3LYP/6-311++G(d,p) (in parentheses) levels.

BP86 calculations predict that **1** ($^3\text{A}'$, C_s , $R_{\text{C-O}} = 1.289\text{ Å}$, $\nu_{\text{C-O}} = 1330.9\text{ cm}^{-1}$) has a structure similar to but smaller $R_{\text{C-O}}$ and higher $\nu_{\text{C-O}}$ than those of the analogous $\text{Sc}_2[\eta^2(\mu_2\text{-C,O})]$ ($^1\text{A}'$, C_s , 1.320 Å , 1237.6 cm^{-1}).^[4] The $R_{\text{C-O}}$ value of **1** is larger than that of $\text{OTi}(\eta^2\text{-CO})$ (1.246 Å).^[12] In comparison with **1**, **2** [$^3\text{A}_2$, C_{2v} , 1.288 Å , 1332.6 cm^{-1} (B_2)] is predicted to have longer Ti–Ti, Ti–C, and Ti–O bonds but almost the same $R_{\text{C-O}}$.

For a trititanium cluster, a side-on-bonded CO ligand may have two possible coordination forms: $\eta^2(\mu_3\text{-C},\mu_2\text{-O})$ and $\eta^2(\mu_2\text{-C},\text{O})$. Our BP86 calculations show that the *cyclo*- $\text{Ti}_3[\eta^2(\mu_3\text{-C},\mu_2\text{-O})]$ ($^3\text{A}'$, C_s , 1.364 Å , 1099.5 cm^{-1}) and *cyclo*- $\text{Ti}_3[\eta^2(\mu_3\text{-C},\mu_2\text{-O})]_2$ ($^1\text{A}'$, C_{2v} , 1.371 Å , 1064.2 cm^{-1}) molecules do not fit the observations, as their calculated $\nu_{\text{C-O}}$ values are much lower than the observed frequencies for $\text{Ti}_3(\text{CO})$ (1253.3 cm^{-1}) and $\text{Ti}_3(\text{CO})_2$ (1189.9 cm^{-1}). Calculations at

the same level show that the planar $cyclo\text{-Ti}_3[\eta^2(\mu_2\text{-C,O})]$ (**3**) molecule (${}^3A''$, C_3 , 1.296 Å, 1302.7 cm^{-1}) and the planar $cyclo\text{-Ti}_3[\eta^2(\mu_2\text{-C,O})]_2$ (**4**) molecule [3B_1 , C_{2v} , 1.291 Å, 1316.0 cm^{-1} (B_2)] (Figure 3) fit the experimental results well (Tables 1 and 2).^[8] For **4**, the calculated symmetric C–O stretching mode (A_1 , 1359.8 cm^{-1} , 45 km mol^{-1}) has an intensity much lower than the antisymmetric one (B_2 , 1316.0 cm^{-1} , 731 km mol^{-1}) (Table S1 in Supporting Information), in agreement with the absence of this A_1 absorption in the IR spectra. By comparing **1** with **3** and **2** with **4**, it is found that addition of the third Ti atom to Ti_2 to form a triangular Ti_3 cluster leads to the lengthening of C–O bonds, which corresponds to weakening of the C–O bond and therefore to lower $\nu_{\text{C-O}}$, in agreement with the observations.

As a Ti cluster carrying three side-on-bonded CO ligands should be considered for the 1397.6 cm^{-1} absorption, we first performed BP86 calculations on possible isomers of $\text{Ti}_2(\text{CO})_3$, which predict that its most stable isomer (3A_1 , C_{3v}) exhibits IR absorptions at 1432.1 and 1357.7 cm^{-1} with intensities of 152 and 502($\times 2$) km mol^{-1} , respectively. The prediction does not match the observation of a single IR absorption at 1397.6 cm^{-1} , and this leads to the conclusion that $\text{Ti}_2(\text{CO})_3$ should be excluded. Calculations at the same level revealed that the planar $cyclo\text{-Ti}_3[\eta^2(\mu_2\text{-C,O})]_3$ (**5**) molecule having a 1A_1 ground state with C_{3h} symmetry (Figure 3) nicely fits the observations for this tricarbonyl species (scale factor 0.967). Species **5** [1A_1 , C_{3h} , 1445.9 cm^{-1} (E')] consists of an equilateral Ti_3 triangle with $R_{\text{Ti-Ti}} = 2.732$ Å, much longer than in the naked Ti_3 cluster^[13] or in **3** or **4**, and three equivalent side-on-bonded CO units with $R_{\text{C-O}} = 1.259$ Å, the shortest among $\text{Ti}_3(\text{CO})_n$ ($n = 1-3$), forming a planar windmill-like molecule. It lies 44.55 kcal mol^{-1} lower in energy than the planar CO-bridged $cyclo\text{-Ti}_3(\mu\text{-CO})_3$ molecule with D_{3h} symmetry, which has three imaginary vibrational frequencies. In addition, the cyclic $\text{Ti}_3(\text{CO})_3$ isomer with terminally bonded CO ligands and D_{3h} symmetry exhibits no geometry convergence, and the removal of symmetry restrictions in the optimization procedure results in a nonplanar structure with C_1 symmetry [$\nu_{\text{C-O}} = 1500.5$ (734), 1450.9 (464), and 1108.2 cm^{-1} (119 km mol^{-1})], which lies 14.75 kcal mol^{-1} higher in energy than **5**. We also performed DFT calculations on other electronic states for the planar C_{3h} $cyclo\text{-Ti}_3[\eta^2(\mu_2\text{-C,O})]_3$ molecule and found that the triplet state exhibits no geometry convergence, and the relative triplet energy at the singlet geometry is predicted to be 9.37 kcal mol^{-1} higher. Species **5** has an $\dots(a')^2(e')^4(e'')^4(a'')^2(a'')^2(e'')^4$ electronic configuration; the doubly degenerate HOMO consists of the π orbitals localized on the Ti–C–Ti subunits, and the HOMO–1 is the delocalized π orbital mainly involving the Ti_3C_3 unit (Figure 4). It is noted that the LUMO is quite low in energy (HOMO–LUMO energy gap: 13.81 kcal mol^{-1}).

Interestingly, theoretical examination of **5** reveals that this molecule may have antiaromatic character. Recently, aromaticity^[14,15] has been extended by gas-phase observations to main-group metal clusters such as Al_4^{2-} , Al_4^{4-} , Si_4^{2+} , Si_4 , Si_4^{2-} , Sn_6^{2-} , and Hg_4^{6-} , which have stimulated several theoretical investigations and heated discussions.^[16] One of the useful approaches to the characterization of aromaticity and antiaromaticity is analysis of the nucleus-independent chemical

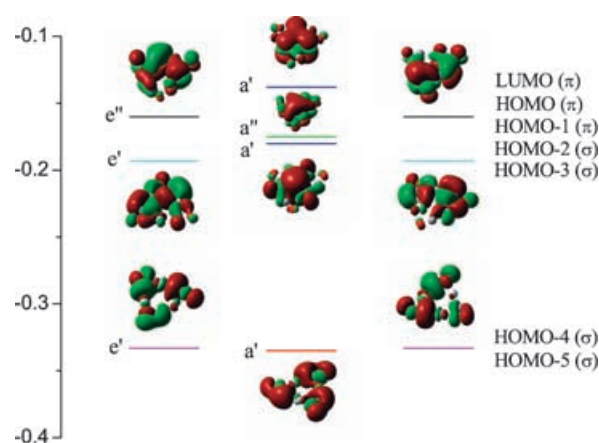


Figure 4. Molecular orbital pictures of singlet $cyclo\text{-Ti}_3[\eta^2(\mu_2\text{-C,O})]_3$ showing the LUMO and the HOMOs down to the fifth valence molecular orbital from the HOMO. HOMO, HOMO–3, and HOMO–4 each consist of degenerate pairs, both of which are shown here.

shift (NICS) on the basis of the magnetic criterion, in which a negative NICS corresponds to aromaticity and a positive NICS to antiaromaticity.^[17] Calculations on **5** at the gauge-including atomic orbital (GIAO) BP86/6-311 + + G(d,p) level show that the NICSs at the Ti_3 ring center and 1 Å above are 23.4 and 14.8, respectively, and thus indicate significant antiaromaticity. The corresponding values for benzene calculated at the same level are -7.7 and -10.1 . Further calculations to clarify the source of the NICS value of **5** by way of current density plots and dissected NICS data are in progress and will be reported in a subsequent full paper.

In summary, FTIR spectroscopy and calculations revealed the novel planar windmill-like $cyclo\text{-Ti}_3[\eta^2(\mu_2\text{-C,O})]_3$ molecule exhibiting antiaromatic character as a new example of transition metal cluster compounds having aromaticity or antiaromaticity. This molecule is generated, along with other side-on-bonded mono- and polycarbonyl di- and trititanium clusters, from the reaction of laser-ablated Ti atoms with CO in a solid argon matrix. All of these molecules show unusually low C–O stretching frequencies and thus represent a new class of metal carbonyls with extremely weakened C–O bonding. It is possible that further development in the concept of aromaticity and antiaromaticity in transition-metal systems, through matrix-isolation and theoretical investigations, will lead to the discovery of new classes of compounds or new insights into the electronic structures and chemical bonding of transition-metal cluster compounds.

Experimental Section

Matrix-isolation IR spectroscopy: The experimental setup for laser ablation and matrix-isolation IR spectroscopy was similar to those in previous reports.^[5] Briefly, Ti atoms ablated with the Nd:YAG laser fundamental (1064 nm, 10 Hz repetition rate) were codeposited with CO in excess argon onto a CsI window at 7 K. IR spectra were recorded on a BIO-RAD FTS-6000e spectrometer at 0.5 cm^{-1} resolution by using a liquid-nitrogen-cooled HgCdTe (MCT) detector for the range of 5000–400 cm^{-1} . Samples were annealed at different temperatures and subjected to broadband irradiation ($\lambda > 250$ nm) from a high-pressure mercury arc lamp (Ushio, 100 W).

Calculations: DFT calculations were performed to predict the structures and vibrational frequencies of the observed reaction products with the Gaussian03 program.^[11] The BP86 density functional was used with 6-311++G(d,p) basis sets for C and O atoms, and the all-electron set of Wachters and Hay as modified by Gaussian03 for Ti atoms. Geometries were fully optimized and vibrational frequencies were calculated with analytical second derivatives. Previous investigations have shown that the use of BP86 can provide reliable information for titanium carbonyls, such as IR frequencies, relative absorption intensities, and isotopic shifts.^[9] For comparison, calculations were also performed with the hybrid B3LYP functional. Molecular orbitals were generated with GaussView.

Received: January 31, 2005
 Revised: April 21, 2005
 Published online: June 9, 2005

Keywords: antiaromaticity · cluster compounds · density functional calculations · IR spectroscopy · matrix isolation

- [1] F. A. Cotton, G. Wilkinson, *Advanced Inorganic Chemistry*, 4th ed., Wiley, New York, **1980**, p. 1049.
- [2] D. W. Moon, S. L. Bernasek, D. J. Dwyer, J. L. Gland, *J. Am. Chem. Soc.* **1985**, *107*, 4363; N. D. Sinn, T. E. Madey, *Phys. Rev. Lett.* **1984**, *53*, 2481; F. M. Hoffmann, R. A. de Paola, *Phys. Rev. Lett.* **1984**, *52*, 1697.
- [3] F. A. Cotton, *Prog. Inorg. Chem.* **1976**, *21*, 1, and references therein; F. A. Cotton, B. A. Frenz, L. Kruczynski, *J. Am. Chem. Soc.* **1973**, *95*, 951; M. Manassero, M. Sansoni, G. Longoni, *J. Chem. Soc. Chem. Commun.* **1976**, 919; W. A. Herrmann, H. Biersack, M. L. Ziegler, K. Weidenhammer, R. Siegel, D. Rehder, *J. Am. Chem. Soc.* **1981**, *103*, 1692; R. Colton, M. J. McCormick, *Coord. Chem. Rev.* **1980**, *31*, 1.
- [4] L. Jiang, Q. Xu, *J. Am. Chem. Soc.* **2005**, *127*, 42.
- [5] T. R. Burkholder, L. Andrews, *J. Chem. Phys.* **1991**, *95*, 8697; M. F. Zhou, N. Tsumori, L. Andrews, Q. Xu, *J. Phys. Chem. A* **2003**, *107*, 2458; L. Jiang, Q. Xu, *J. Chem. Phys.* **2005**, *122*, 034505.
- [6] M. F. Zhou, L. Andrews, C. W. Bauschlicher, Jr., *Chem. Rev.* **2001**, *101*, 1931; J. Li, B. E. Bursten, B. Y. Liang, L. Andrews, *Science* **2002**, *295*, 2242; L. Andrews, X. F. Wang, *Science* **2003**, *299*, 2049.
- [7] M. F. Zhou, N. Tsumori, Z. H. Li, K. N. Fan, L. Andrews, Q. Xu, *J. Am. Chem. Soc.* **2002**, *124*, 12936; M. F. Zhou, Q. Xu, Z. X. Wang, P. von R. Schleyer, *J. Am. Chem. Soc.* **2002**, *124*, 14854.
- [8] See Supporting Information.
- [9] G. V. Chertihin, L. Andrews, *J. Am. Chem. Soc.* **1995**, *117*, 1595; M. F. Zhou, L. Andrews, *J. Phys. Chem. A* **1999**, *103*, 5259; R. Busby, W. Klotzbücher, G. A. Ozin, *Inorg. Chem.* **1977**, *16*, 822.
- [10] J. H. Darling, J. S. Ogden, *J. Chem. Soc. Dalton Trans.* **1972**, 2496.
- [11] Gaussian03 (Revision B.04), M. J. Frisch, G. W. Trucks, H. B. Schlegel, G. E. Scuseria, M. A. Robb, J. R. Cheeseman, J. A. Montgomery, Jr., T. Vreven, K. N. Kudin, J. C. Burant, J. M. Millam, S. S. Iyengar, J. Tomasi, V. Barone, B. Mennucci, M. Cossi, G. Scalmani, N. Rega, G. A. Petersson, H. Nakatsuji, M. Hada, M. Ehara, K. Toyota, R. Fukuda, J. Hasegawa, M. Ishida, T. Nakajima, Y. Honda, O. Kitao, H. Nakai, M. Klene, X. Li, J. E. Knox, H. P. Hratchian, J. B. Cross, C. Adamo, J. Jaramillo, R. Gomperts, R. E. Stratmann, O. Yazyev, A. J. Austin, R. Cammi, C. Pomelli, J. W. Ochterski, P. Y. Ayala, K. Morokuma, G. A. Voth, P. Salvador, J. J. Dannenberg, V. G. Zakrzewski, S. Dapprich, A. D. Daniels, M. C. Strain, O. Farkas, D. K. Malick, A. D. Rabuck, K. Raghavachari, J. B. Foresman, J. V. Ortiz, Q. Cui, A. G. Baboul, S. Clifford, J. Cioslowski, B. B. Stefanov, G. Liu, A. Liashenko, P. Piskorz, I. Komaromi, R. L. Martin, D. J. Fox, T. Keith, M. A. Al-Laham, C. Y. Peng, A. Nanayakkara, M. Challacombe, P. M. W. Gill, B. Johnson, W. Chen, M. W. Wong, C. Gonzalez, J. A. Pople, Gaussian, Inc., Pittsburgh, PA, **2003**.
- [12] M. F. Zhou, L. Andrews, *J. Phys. Chem. A* **1999**, *103*, 2066.
- [13] M. Castro, S. R. Liu, H. J. Zhai, L. S. Wang, *J. Chem. Phys.* **2003**, *118*, 2116.
- [14] Thematic Issue on Aromaticity (Guest Ed.: P. von R. Schleyer), *Chem. Rev.* **2001**, *101*(5).
- [15] P. J. Garratt, *Aromaticity*, Wiley, New York, **1986**; V. J. Minkin, M. N. Glukhovtsev, B. Y. Simkin, *Aromaticity and Antiaromaticity; Electronic and Structural Aspects*, Wiley, New York, **1994**.
- [16] X. Li, A. E. Kuznetsov, H. F. Zhang, A. I. Boldyrev, L. S. Wang, *Science* **2001**, *291*, 859; Z. F. Chen, C. Corminboeuf, T. Heine, J. Bohmann, P. von R. Schleyer, *J. Am. Chem. Soc.* **2003**, *125*, 13930; A. E. Kuznetsov, K. A. Birch, A. I. Boldyrev, X. Li, A. I. Zhai, L. S. Wang, *Science* **2003**, *300*, 622; A. E. Kuznetsov, J. D. Corbett, L. S. Wang, A. I. Boldyrev, *Angew. Chem.* **2001**, *113*, 3473; *Angew. Chem. Int. Ed.* **2001**, *40*, 3369; H. J. Zhai, A. E. Kuznetsov, A. I. Boldyrev, L. S. Wang, *ChemPhysChem* **2004**, *5*, 1885.
- [17] P. von R. Schleyer, C. Maerker, A. Dransfeld, H. Jiao, N. J. R. van Eikema Hommes, *J. Am. Chem. Soc.* **1996**, *118*, 6317; P. von R. Schleyer, H. Jiao, N. J. R. van Eikema Hommes, V. G. Malkin, O. L. Malkina, *J. Am. Chem. Soc.* **1997**, *119*, 12669.